Published in final edited form as:
Brain. 2003 August ; 126(0 8): . doi:10.1093/brain/awg184.

Dopaminergic drug effects on physiological connectivity in a human cortico-striato-thalamic system

G. D. Honey[1], **J. Suckling**[1], **F. Zelaya**[3], **C. Long**[3], **C. Routledge**[2], **S. Jackson**[3], **V. Ng**[3], **P. C. Fletcher**[1], **S. C. R. Williams**[3], **J. Brown**[2], and **E. T. Bullmore**[1,3]

[1]Department of Psychiatry, University of Cambridge, London, UK

[2]GlaxoSmithKline Clinical Research Unit, ACCI, Cambridge, London, UK

[3]Institute of Psychiatry, King's College, London, UK

Summary

Cortico-striato-thalamic (CST) systems are anatomical substrates for many motor and executive functions and are implicated in diverse neuropsychiatric disorders. Electrophysiological studies in rats, monkeys and patients with Parkinson's disease have shown that power and coherence of low frequency oscillations in CST systems can be profoundly modulated by dopaminergic drugs. We combined functional MRI with correlational and path analyses to investigate functional and effective connectivity, respectively, of a prefronto-striato-thalamic system activated by object location learning in healthy elderly human subjects (n = 23; mean age = 72 years). Participants were scanned in a repeated measures, randomized, placebo-controlled design to measure modulation of physiological connectivity between CST regions following treatment with drugs which served both to decrease (sulpiride) and increase (methylphenidate) dopaminergic transmission, as well as non-dopaminergic treatments (diazepam and scopolamine) to examine non-specific effects. Functional connectivity of caudate nucleus was modulated specifically by dopaminergic drugs, with opposing effects of sulpiride and methylphenidate. The more salient effect of sulpiride was to increase functional connectivity between caudate and both thalamus and ventral midbrain. A path diagram based on prior knowledge of unidirectional anatomical projections between CST components was fitted satisfactorily to the observed inter-regional covariance matrix. The effect of sulpiride was defined more specifically in the context of this model as increased strength of effective connection from ventral midbrain to caudate nucleus. In short, we have demonstrated enhanced functional and effective connectivity of human caudate nucleus following sulpiride treatment, which is compatible both with the anatomy of ascending dopaminergic projections and with electrophysiological studies indicating abnormal coherent oscillations of CST neurons in parkinsonian states.

Keywords

cortico-striato-thalamic loops; functional/effective connectivity; pharmacological MRI; dopamine; path analysis

Correspondence to: Professor Edward Bullmore, University of Cambridge, Brain Mapping Unit, Department of Psychiatry, Addenbrooke's Hospital, Cambridge CB2 2QQ, UK, etb23@cam.ac.uk.

Europe PMC Funders Author Manuscripts

Introduction

An influential model of neurocognitive architecture emphasizes the central importance of cortico-striato-thalamic (CST) circuits. Diverse neuropsychiatric disorders have been attributed to disordered function of CST systems (Robbins, 1990; Owen *et al.*, 1992; Pantelis *et al.*, 1997; Lawrence *et al.*, 1998; Graybiel and Rauch, 2000; Overmeyer *et al.*, 2001). Neuroanatomical studies of non-human primates indicate that a general scheme of cortico-subcortical integration is common to several parallel segregated CST circuits, each of which comprises a specific set of frontal cortical areas and subcortical nuclei, and receives modulatory input to striatum from ascending dopaminergic projections of the substantia nigra compacta in the midbrain (Alexander *et al.*, 1986, 1990; Wichmann and DeLong, 1996; Masterman and Cummings, 1997); see Fig. 1.

Several recent lines of investigation have convergently indicated a key role for dopamine in the modulation of spontaneous, long-memory oscillations in basal ganglia and synchronization or coherence of neuronal activity between components of cortico-striato-thalamic (CST) circuits. For example, extracellular single unit recordings in rats have demonstrated that slow, periodic oscillations in spontaneous activity of basal ganglia neurons are profoundly modulated by administration of the dopamine agonist apomorphine, which increased both the frequency and peak power of oscillation (Ruskin *et al.*, 1999; Walters *et al.*, 2000). Multiple electrode recordings in monkeys have also shown that both power of low frequency (7 and 13 Hz) oscillations and coherence between normally independent pallidal and striatal neurons are increased after treatment with 1-methyl-4-phenyl-1,2,3,6-tetrahydropyridine (MPTP), causing parkinsonism (Bergman *et al.*, 1998; Raz *et al.*, 2000, 2001). In patients studied following neurosurgical treatment for Parkinson's disease, macroelectrode recordings demonstrated low frequency oscillations in globus pallidus and subthalamic nucleus which were highly sensitive to dopaminergic manipulation: administration of the dopamine precursor L-dopa caused increased frequency and phase reversal of coherent oscillation in these nuclei (Brown *et al.*, 2001). Similarly, the frequency and phase of cortico-subthalamic coherent oscillations were modulated in Parkinson's disease patients by administration of L-dopa (Williams *et al.*, 2002). These electrophysiological observations collectively indicate that dopamine plays a critical role in modulating the extent of functional segregation within basal ganglia and between multiple, anatomically parallel cortico-subcortical circuits.

Anatomical and physiological characterization of normal CST systems in humans is obviously not possible by the more direct, but invasive, methods used for this purpose in animal models. However, functional neuroimaging offers the opportunity to investigate frontal-subcortical systems in living, healthy subjects. There has been considerable effort to develop multivariate statistical methods for analysis of correlated physiological activity in human brain systems identified by functional neuroimaging (Bullmore *et al.*, 1996, 2000; McIntosh *et al.*, 1996; Friston *et al.*, 1997, 1999; Worsley *et al.*, 1998; Büchel *et al.*, 1999; Mechelli *et al.*, 2002; Welchew *et al.*, 2002). Such methods have previously been used to examine the interactions between striatum and cortical regions (Toni *et al.*, 2002) and to demonstrate deficits in cortico-cortical interactions in patients with Parkinson's disease (Rowe *et al.*, 2002). To the best of our knowledge, however, they have not hitherto been used either to characterize physiological connectivity between components of human CST circuits or to assess drug effects on functional MRI (fMRI) measures of connectivity in humans or monkeys. Primarily on the basis of prior electrophysiological data (Bergman *et al.*, 1998; Brown *et al.*, 2001), we predicted that physiological connectivity within human CST circuits would be modulated by pharmacological manipulation of dopaminergic transmission. We tested this hypothesis in a randomized, repeated-measures, placebo-

controlled design using fMRI to measure integrated function of a prefronto-striato-thalamic system in healthy, elderly volunteers.

Material and methods

Subjects and study design

Twenty-three healthy, elderly, right-handed volunteers participated in the study. All participants were carefully screened by a structured health questionnaire, full clinical examination and supplementary investigations including ECG, haematology and blood biochemistry, and urine analysis for undeclared drug use. Specifically to exclude significant neurological or psychiatric disorder, participants were also required to have a radiologically normal anatomical MRI examination and a mini-mental state examination score (MMSE) of ≥26 (maximum score = 30); in fact, most participants had MMSE scores of 30 or 29, and only three participants had recorded scores of <28.

Written informed consent was provided by all participants. The study was approved by the Bethlem Royal and Maudsley NHS Trust Ethics (Research) Committee.

We used a randomized, single-blind, placebo-controlled design; for ethical and clinical reasons, one member of the study team was not blind to treatment. Participants were scanned using fMRI on three separate occasions at 14-day intervals. To habituate participants to the magnetic resonance scanning environment, and to acquire anatomical MRI data, participants were also briefly scanned as part of their screening assessment before starting the fMRI study.

The study comprised two treatment arms: across the three sessions, a ‘dopaminergic treatment group’ received oral placebo, methylphenidate 20 mg (a dopamine reuptake inhibitor used clinically in the treatment of attention deficit hyperactivity disorder) and sulpiride 400 mg (a selective antagonist at dopamine D2 receptors used clinically as an anti-psychotic). The ‘non-dopaminergic treatment group’ received placebo, subcutaneous scopolamine 0.35 mg (a muscarinic M2 receptor antagonist, widely used as a pre-operative medication in general surgery) and oral diazepam 5 mg (a γ-aminobutyric acid $GABA_A$ receptor agonist, widely used as an anxiolytic and hypnotic). The order of treatments was randomized within groups.

Half the sample (Group A; $n = 12$; four male, eight female; mean age = 69.75 years; age range 61–80 years) was randomly assigned to the dopaminergic treatment group. The other half of the sample (Group B; $n = 11$; four male, seven female; mean age = 75 years; age range 70–80 years) was assigned to the non-dopaminergic treatment group. To control for different modes of administration of active compounds in Group B, six of these participants received an oral placebo and five had a subcutaneous injection of placebo (normal saline).

To accommodate the different pharmacokinetic profiles of these four active compounds, they were administered at different times before scanning to ensure effective and stable plasma concentrations during fMRI: sulpiride and diazepam were given 180 min prior to scanning; and methylphenidate, scopolamine and placebo were given 90 min before scanning. All drugs were well tolerated at these doses and all participants completed the scanning protocol successfully.

This design allowed us to assess changes in physiological connectivity within the CST system in the context of opposing pharmacological manipulations, which served to both increase (methylphenidate) and decrease (sulpiride) dopaminergic transmission. We reasoned that modulation of connectivity, which reflected this bipolar pharmacological

Europe PMC Funders Author Manuscripts

manipulation, could be compellingly related to specific effects on the dopaminergic system, particularly if observed in the absence of similar effects from treatments which do not directly modulate dopamine (scopolamine and diazepam).

fMRI data acquisition

Gradient-echo echoplanar T_2*-weighted images depicting blood oxygen level dependent (BOLD) contrast were acquired at 1.5 Tesla from 16 non-contiguous near axial planes, with the following parameters: TE (echo time) = 40 ms; TR (repetition time) = 2000 ms; flip angle = 70°; slice thickness = 7 mm; inter-slice gap = 0.7 mm; in-plane resolution = 3.75 mm; matrix size = 64 × 64. To facilitate later registration of fMRI data in standard space, a higher resolution echo planar imaging (EPI) dataset comprising 43 near-axial slices was also acquired with the following parameters: TR = 6000 ms; TE = 40 ms; TI (inversion time) = 1500 ms; flip angle = 90°; slice thickness = 3 mm; inter-slice gap = 0.3 mm; matrix size = 128 × 128.

Object–location learning

The object–location learning paradigm used in this study was selected on the basis of prior data indicating that a load-adaptive response to this task was demonstrated by a fronto-striato-thalamic system (Bullmore *et al.*, 2003). A graded block design was used to optimize the efficiency of regression model parameter estimation. Object–location learning trials (Fig. 2) were presented in 24 s blocks, alternating with 24 s blocks of cross-hair fixation; this cycle was repeated eight times for a total experimental duration of 6 min 24 s. Cognitive load was graded by alternately presenting blocks of trials at one of two possible levels of difficulty. In an ‘easy’ trial, a set of two stimuli (highly discriminable coloured shapes) was shown for 1500 ms either side (left and right) of a central crosshair, followed by 500 ms of central crosshair alone, followed by central presentation of one of the two original stimuli for 2000 ms. The subject was trained to move a joystick in the direction of the location (left or right) originally occupied by the central stimulus. A ‘difficult’ trial was exactly the same except that a set of four stimuli was initially arrayed around the central crosshair. For each level of difficulty, the same set of stimuli was repeatedly presented in the same locations across all trials. For both levels of difficulty, trial duration was 4 s, i.e. there were six trials per block. Subjects were informed immediately by visual feedback whether the response to each trial was correct or incorrect, and accuracy and reaction time of response were recorded by pressing the right-handed button during scanning.

Activation mapping

After correction of temporal offsets due to multislice acquisition and head movement-related effects in the fMRI time series at each voxel (Bullmore *et al.*, 1999b), a linear regression model was fitted by least squares to estimate experimentally induced signal changes in the context of residual autocorrelation with 1/f-like or long-memory structure (Bullmore *et al.*, 2001). Regression analysis modelled the difference between the two levels of difficulty of the activation condition, which characterized cognitive load response [orthogonal periodic and linear time-related effects were also modelled, but these are not reported further here; see Bullmore *et al.* (2003) for details]. Prior to model fitting, each column of the design matrix was convolved by a pair of Poisson kernels (λ = 4 or 8 s) to model locally variable haemodynamic response functions. Statistical maps representing the standardized effects for each individual under each drug treatment were registered in the standard space of Talairach and Tournoux (1988) by an affine transformation to a template image (Brammer *et al.*, 1997).

Generic activation maps indicating areas of significant response following placebo treatment were created by a permutation test of the median standardized effect at each suprathreshold

cluster (Brammer *et al.*, 1997; Bullmore *et al.*, 1999a). Cluster level analysis involved applying a preliminary probability threshold ($P < 0.05$) to the voxel statistic maps and setting all subthreshold voxels to zero, thus creating a set of suprathreshold voxel clusters that are spatially contiguous in 3D. The sum of suprathreshold voxel statistics or 'mass' of each cluster was then tested by a permutation test at each cluster (Bullmore *et al.*, 1999a). A one-tailed clusterwise probability of type 1 error $P \leq 0.01$ was adopted; at this size of significance threshold, we expect less than one false positive test over all the clusters tested in each map. The primary aim of this activation mapping was to identify the anatomical coordinates of time series demonstrating significant load response, in the expectation that cortical and subcortical regions showing a shared pattern of response to the experimental task could be regarded as constituents of a functionally integrated CST circuit and might therefore provide a reasonable basis for modelling hypothesized drug effects on CST connectivity. However, we note that activation mapping is not an essential prerequisite for connectivity analysis. One could, in principle, select time series based on inspection of non-thresholded statistical parameter maps, selecting series from regions with local maxima of voxel statistics; or one could use purely anatomical criteria to sample series from regions known *a priori* to constitute integrated CST circuits.

Regional time series analysis

Regional mean fMRI time series were sampled from each individual under each treatment condition by averaging the time series extracted from a generically activated index voxel (one for each region) and its eight nearest neighbours in the axial (x–y) plane. Time series data corresponding to the activation condition at each level were then separately concatenated as described by Honey *et al.* (2002) to create two within-task series, one for each level of load, at each region. To do this, we assumed a mean haemodynamic delay of 4 s, i.e. 2 TR, between the onset and offset of each activation condition and the corresponding onset and offset of related physiological response (Horwitz *et al.*, 2000). For the easy level of difficulty ($n = 2$ items) condition, there were $T = 52$ time points comprising each regional within-task series; for the higher difficulty level ($n = 4$ items), there were $T = 50$ time points per series. This was because one of the epochs of this task was presented last in the experimental sequence of conditions and therefore truncated by (4 s = 2 TR) correction for haemodynamic delay.

This method of time series 'splicing' to obtain concatenated segments of data specific to a particular task condition or level of difficulty has the advantage of conceptual simplicity and is suitable for both correlational and path analysis of within-task covariance. An alternative approach, which has been elegantly used in path analysis of task-specific effects of one (source) region on another (target) region, is to compute the product of the haemodynamically convolved input function for the task condition of interest with the time series of the source region and then to use this interaction term or moderator variable as a predictor of variance in the target region (Büchel and Friston, 1997). Both approaches will typically involve making some assumptions about the haemodynamically mediated delay between onset of task presentation and onset of task related fMRI signal.

Physiological connectivity analysis

Overview and nomenclature—Analysis of physiological connectivity in brain systems has been subdivided into analysis of functional connectivity and effective connectivity (Gerstein and Perkel, 1969; Gerstein *et al.*, 1989; Friston *et al.*, 1993). Functional connectivity analysis refers to the estimation of simple statistical measures of association or dependency between two neurophysiological time series recorded from different voxels or spatially distinct regions. Effective connectivity analysis involves the more ambitious attempt to model mechanistic effects of one brain region on another, mediated by known

anatomical connections between them. Thus functional connectivity is essentially statistical, whereas effective connectivity is a hybrid concept incorporating prior anatomical data and some model of causal or at least unidirectional interactions between brain regions. Here we have applied methods for analysis of both functional and effective connectivity to the same data. The added value of this dual approach is that correlational analysis of functional connectivity is a conceptually simple way of identifying drug effects on brain systems, but is not informed by prior anatomic knowledge; whereas path analysis of effective connectivity is conceptually and operationally more complex, but it can provide a more specific representation of drug effects in the context of prior knowledge of CST anatomy and neurochemistry. Thus, we intended that the relatively model-free results of correlational analysis could substantiate and corroborate the more informed but more elaborately modelled results of path analysis.

To assess functional connectivity, we estimated the correlations between each pair of five prefrontal cortical, striatal, thalamic and midbrain regions for each individual under each drug treatment. To assess effective connectivity, we specified a path model based on extensive prior knowledge of CST structure in primates, validated this model for human data in two independent groups of subjects treated with placebo, and fitted it to each individual's inter-regional covariance matrix under each drug treatment. To make inferences about pharmacological effects on connectivity, we used our indices of coupling (Z-transformed correlation coefficients and path coefficients) as dependent variables in standard analyses of variance looking for condition and treatment effects. We subsequently elaborated these analyses by including some behavioural measures as a covariate. Note that this approach corresponds to a second level analysis if we treat the coupling indices as summary statistics from a first level analysis. In this sense our inferences are, quite properly, made in relation to inter-subject variability, which is not the case for inference made on the basis of correlations or path coefficients estimated from group averaged regional fMRI time series; see Rowe *et al.* (2002) and Lawrie *et al.* (2002) for similar prior approaches to second level connectivity analysis. Further statistical details are provided below.

Functional connectivity—We used Pearson's correlation coefficient as a measure of functional connectivity. We constructed a (5 × 5) within-task, inter-regional correlation matrix for each subject under each drug treatment. The correlation coefficient for the *i*th and *j*th regions, $r_{i,j}$, was transformed to a standard Normal distribution using Fisher's *r*-to-*z* transformation:

$$Z_{i,\,j}=\frac{1}{2}\ln\left(1+r_{i,\,j}\right)/\left(1-r_{i,\,j}\right) \quad (1)$$

To estimate drug effects on functional connectivity, we used a linear mixed effects model for normalized inter-regional correlations, treating subject as a random effect and drug treatment and task difficulty as fixed effects, i.e.

$$z_{kmn}=\mu+\beta_m+\gamma_n+b_k+\varepsilon_{kmn} \quad (2)$$

where z_{kmn} is the standardized inter-regional correlation coefficient (for the ith and *j*th regions) in the *k*th subject under the *m*th treatment and *n*th load condition; μ is the overall mean inter-regional correlation; β_m is the fixed effect of the *m*th treatment; γ_n is the fixed effect of the *n*th difficulty condition; b_k is a random variable representing the deviation of the *k*th subject from the population mean inter-regional correlation, $b_k \sim N\left(0, \sigma_b^2\right)$ and ε_{kmn} is a normally distributed error term with zero mean and variance σ_ε^2.

Testing the null hypothesis that the main effect of treatment was zero for each of 10 inter-regional correlations possible between $p = 5$ regions of interest implied 10 significance tests which were conservatively adjusted for multiple comparisons using the Bonferroni correction.

Effective connectivity—We also wanted to estimate drug effects on physiological connectivity in the context of an anatomically informed model for CST function. To do this, we used path analysis or structural equation modelling. For a general introduction to path analysis see Loehlin (1987), Glymour *et al.* (1987) or Bollen (1989); for prior applications to functional neuroimaging, see McIntosh *et al.* (1994, 1996), Büchel and Friston (2000), Bullmore *et al.* (2000) or Gitelman *et al.* (2002); and for a prior application to genetic neuroimaging, see Wright *et al.* (2002).

Briefly, path analysis of fMRI data requires an inter-regional covariance matrix and a path diagram summarizing the anatomically permissible interactions between regions. The path coefficients quantifying the strength of effective connection between each pair of linked regions in the diagram are estimated so as to minimize the discrepancy between the observed covariance matrix and the covariance matrix predicted by the diagram. If the path model provides a good account of the data, this discrepancy will be small and quite likely under the null hypothesis. More formally, the maximum likelihood method of path model estimation finds the minimum discrepancy, F, between the observed covariance matrix, C, and the matrix predicted by the path model, $\Sigma(q)$, i.e. $F = \min\{f[C, \Sigma(q)]\}$. Under the null hypothesis that the population covariance matrix $\Sigma = \Sigma(q)$, the minimum value of the discrepancy function multiplied by the number of independent observations on each variable n is distributed approximately as χ^2 on k–q degrees of freedom, i.e. $nF \sim \chi^2_{k-q}$, where q is the number of path coefficients to be estimated and $k = \frac{1}{2}p(p+1) = 15$ is the number of regional variances and inter-regional covariances on the basis of which to estimate them. Path models that provide a good account of the observed data will be associated with small minima of the discrepancy function, F, and correspondingly large probabilities ($P > 0.1$) under the null hypothesis. Model performance can also be evaluated by various other indices: good models will generally have low values for the root mean square error of approximation (RMSEA) and high values for Bollen's (parsimonious) fit index (BFI) ($0 < BFI < 1$).

Model specification—An important incentive in applying path analysis to pharmacological fMRI data on CST systems is that the anatomy and neurochemistry of these systems has been especially well established in animal models (for review see Alexander *et al.*, 1986, 1990; Afifi and Bergman, 1998; Mega and Cummings, 2001). Moreover, many of the anatomical connections in these circuits are known to be unidirectional, which usefully constrains specification of parsimonious and identifiable path models. Drawing on these and other prior sources, we specified a series of unidirectional connections from dorsal prefrontal cortex to caudate nucleus (Selemon and Goldman-Rakic, 1985), from caudate nucleus to thalamus, and then from thalamus back to dorsal prefrontal cortex bilaterally (Kievit and Kuypers, 1977; Giguere and Goldman-Rakic, 1988; Dermon and Barbas, 1994). This basic loop does not include globus pallidus, which is implicated in both direct and indirect striato-thalamic connections (Kim *et al.*, 1976; Parent *et al.*, 1984; Ilinsky *et al.*, 1985), because there was no evidence of significant generic activation of globus pallidus in these data. In addition to these core features of the dorsolateral prefrontal CST circuit, our path diagram incorporated reciprocal connections between a generically activated region of ventral midbrain (subsuming the substantia nigra) and each ipsilateral component of the circuit. There is anatomical evidence for direct reciprocal connections between midbrain and caudate nucleus and between midbrain and prefrontal cortex, as well as indirect connections

between midbrain and thalamus via the subthalamic nucleus. Finally, we included reciprocal connections between bilaterally homologous regions of prefrontal cortex in view of the dense anatomical connectivity between right and left frontal cortical areas (Pandya and Yeterian, 1990; McGuire *et al.*, 1991) and prior evidence for enhanced physiological connectivity in prefronto-prefrontal circuits under conditions of high cognitive load (Honey *et al.*, 2002).

In short, the complete path diagram (Fig. 3) comprises five unidirectional connections constituting a prefronto-striato-thalamic circuit; six bidirectional connections allowing possible interactions between components of this circuit and ipsilateral midbrain nuclei; and two connections allowing prefronto-prefrontal interactions. The total number of path coefficients to be estimated q = 13.

Path model estimation and evaluation—To evaluate this model, we first fitted it to the group mean inter-regional covariance matrix for subjects in treatment Group A. This matrix was constructed simply by averaging the regional fMRI time series over all subjects following placebo treatment in Group A and then estimating the covariances between group mean regional time series; see Table 1. Effective degrees of freedom and residual variances for each group mean time series were estimated by principal component analysis as described previously (Bullmore *et al.*, 2000; Honey *et al.*, 2002); Table 1. To explore the replicability of model fit, we also constructed a group mean covariance matrix over all the subjects following placebo treatment in Group B and separately fitted the same path diagram to this matrix.

To estimate the effects of drug treatment on effective connections specified by this path model, we fitted the model separately to the inter-regional covariance matrix constructed for each individual under each drug treatment and load condition in both Groups A and B. We then fitted a linear mixed effects model formally identical to Eqn 2, incorporating drug treatment and task difficulty as fixed effects and subject as a random effect, with path coefficients rather than normalized correlation coefficients as the dependent variable. Significance tests on model parameters were corrected for multiple comparisons by a Bonferroni procedure.

All path models were estimated using maximum likelihood methods implemented in LISREL software, version 8 (Jöreskog and Sörbom, 1996) and S-Plus (Venables and Ripley, 2002).

Effects of time and behavioural performance—To test the hypothesis that drug effects on functional and effective connectivity might be explicable in terms of drug effects on behavioural measures of task performance, we extended the linear mixed effects model (Eqn 2) to include as a covariate the mean latency (reaction time) of object location learning by each individual at each level of difficulty and drug treatment, and an interaction between reaction time and drug treatment. This model was fitted identically to correlation and path coefficients treated separately as dependent variables.

We were also concerned to test the hypothesis that drug effects on connectivity might vary dynamically in the course of repeated presentation of trials in the object location learning experiment. To address this possibility, we estimated inter-regional correlation and path coefficients using only the first four and last four blocks of trials and fitted the linear mixed effects model (Eqn 2) to these data, substituting the main effect of time (early or late) for the main effect of load (two- or four-item learning) in the original model; in this analysis, we also estimated an interaction between time and drug treatment.

Results

Behavioural data

There were highly significant effects of both difficulty (number of items) and practice (block number) on latency of task performance during scanning after placebo treatment: main effect of number of items, [$F(1,23) = 100.4$, $P < 0.01$]; and main effect of block number, [$F(3,21) = 10.79$, $P < 0.001$]. There were also significant effects of both difficulty and practice on accuracy of task performance measured during scanning after placebo: main effect of number of items, [$F(1,23) = 18.8$, $P < 0.001$]; and main effect of block number, [$F(3,21) = 4.5$, $P = 0.014$]. The interaction between difficulty and practice was not significant for either latency or accuracy.

Neither the main effect of drug treatment nor the interactive effects of drug × load or drug × block number were significant for accuracy or latency of response in either treatment group.

Generic activation mapping

Combining data from all subjects following placebo treatment, we demonstrated significantly increased activation by increased difficulty of the object–location learning task in a load-responsive system including the following brain regions: left dorsolateral prefrontal cortex, extending into the cingulate gyrus [approximate Brodmann area 9, 46; *x, y, z* Talairach co-ordinates (mm): −24, 24, 28], right dorsolateral prefrontal cortex (Brodmann area 9, 46; 18, 30, 28), caudate nucleus (15, 18, 1), ventro-posterior thalamus (17, 33, 4) and ventral midbrain (22, −30, −4); see Fig. 4]. Regional fMRI time series for right and left dorsolateral prefrontal cortex, caudate nucleus, thalamus and ventral midbrain were extracted from each individual dataset at these coordinates.

Functional connectivity analysis

The group mean correlation and covariance matrices summarized in Table 1 indicate that the components of this fronto-striato-nigro-thalamic system were functionally connected to each other on average over all subjects in Group A and Group B under placebo treatment. The time series activity underpinning inter-regional correlations is illustrated by representative data extracted from caudate nucleus and ventral midbrain in two individuals following placebo treatment in Group A; see Fig. 5.

The effects of drug treatment on individually estimated inter-regional correlation coefficients are summarized in Table 2. Dopaminergic treatments (in Group A) had the most salient effects and these were localized to the functional connections of the caudate nucleus with the thalamus and ventral midbrain. The functional connection between caudate and thalamus demonstrated a significant main effect of dopaminergic drug treatment (after Bonferroni correction for multiple comparisons $P = 0.025$); also, the dopaminergic drug effect on the connection between caudate and midbrain was close to the corrected threshold for significance ($P = 0.057$). For both these connections, the effect of sulpiride was to increase functional connectivity compared with placebo, whereas the effect of methylphenidate was either to decrease functional connectivity compared with placebo (for caudate– midbrain correlation) or neutral with respect to placebo (for caudate–thalamic correlation). There were no significant effects of task difficulty and no effects of scopolamine or diazepam on functional connectivity by this analysis.

Drug effects on inter-regional correlations can also be visualized at the level of fMRI time series extracted from caudate nucleus and ventral midbrain in two individuals following sulpiride and methylphenidate treatment in Group A; see Fig. 5.

Effective connectivity analysis

The path diagram (Fig. 3) provided a good account of the group mean inter-regional covariance matrix for Group A following placebo treatment: $\chi^2(2) = 1.61$, $P = 0.66$; RMSEA = 0, 95% confidence interval (0, 0.14); BFI = 0.98. The same model also provided a good account of the group mean inter-regional covariance matrix for Group B following placebo treatment: $\chi^2(2) = 2.59$, $P = 0.46$; RMSEA = 0, 95% confidence interval (0, 0.26); BFI = 0.94. On this basis, we can conclude that the path diagram provides a reasonable account of the observed covariance structure in two independent groups performing the same task.

The results of linear mixed effects modelling of individually estimated path coefficients are summarized in Table 3. It is notable that some path coefficients were larger, on average, than others: for example, the effective connections from midbrain to caudate and thalamus were strong (significantly non-zero), whereas the effective connections from midbrain to right prefrontal cortex and vice versa were close to zero. The coefficient for the path from caudate to thalamus was also relatively small and this may reflect the departure of our model at this point from the more complex connections, via globus pallidus and other nuclei, intervening anatomically between caudate and thalamus. However, it is also notable that the mean path coefficients are remarkably similar for the two treatment groups, providing an informal indication of the stability of the model and the replicability of these results.

Following correction for multiple comparisons, the only effective connection that was significantly modulated by drug treatment was the projection from ventral midbrain to caudate nucleus in treatment Group A. Here the effect of sulpiride was to increase the strength of effective connection relative to placebo, whereas the effect of methylphenidate was (less saliently) to decrease the strength of effective connection. There were no significant effects of task difficulty and no effects of scopolamine or diazepam on effective connectivity by this analysis.

Effects of time and behavioural performance

There was no significant effect of task performance (reaction time) on any measure of inter-regional connectivity and no significant interaction between task performance and drug treatment. These results indicate that the effects of drug treatment on inter-regional connectivity in this system cannot simply be explained in terms of drug effects on behavioural performance of the task. There was also no significant effect of time on any measure of inter-regional connectivity and no significant interaction between time and drug treatment.

Discussion

We confirmed our hypothetical expectation that dopaminergic drugs would significantly modulate functional and effective connectivity between components of a human CST system, which was supported by the broadly convergent results of two complementary statistical analyses.

We found that a path model of the components of the CST, incorporating unidirectional projections from cortex to thalamus via striatum, provided a good account of the observed covariances between these regions and ventral midbrain. Moreover, our model provided consistently good results when fitted to a second, independent group mean covariance matrix and generated very similar estimates of mean effective connectivity when fitted to the covariance matrices individually estimated for each of 23 subjects in two treatment groups. These results do not, of course, prove that our model is absolutely correct or even the best of all possible path models. More modestly, but still importantly, these results strongly indicate for the first time in humans that it is possible to use detailed prior anatomical knowledge of

CST organization to provide a stable, satisfactory and replicable account of the observed covariance structure in a set of fMRI time series extracted from these regions.

The distinctive value of such a model is illustrated by comparing our results concerning drug effects on functional and effective connectivity. Using both correlation coefficients and path coefficients as our measures of inter-regional connectivity, we were able to show that dopaminergic drugs (sulpiride and methylphenidate) had more salient effects on connectivity than cholinergic (scopolamine) or GABAergic (diazepam) agents. Correlational analysis revealed that dopaminergic drug effects involved particularly the functional connections of the caudate nucleus. Using path analysis, we were able to achieve a more precise localization of this effect, which was most significantly represented in the context of the model by a modulation of the effective connection from ventral midbrain to caudate nucleus. The other main effect of sulpiride demonstrated by correlational analysis was to enhance functional connectivity between caudate and thalamus. This could be interpreted in terms of an effect of striatal dopaminergic input on GABAergic striatopallidal activity, which has been shown by several studies to be reciprocally related to striatal dopamine (Chapman and See, 1996; Opacka-Juffry *et al.*, 1998; Grimm and See, 1998), and mediates a connection between striatal and thalamic nuclei. The functional connection modelled between these two regions using path analysis did not show an effect of dopaminergic manipulation: this likely reflects the imprecision of this aspect of our path model, which did not incorporate intervening paths between caudate and thalamus via the globus pallidus, as significant pallidal activation was not observed in this study. The generalization emergent from both analyses is that striatal connectivity in humans is specifically modulated by dopaminergic drugs; in particular, sulpiride increases connectivity between caudate and other circuit components. It is also interesting, and common to both analyses, that sulpiride and methylphenidate, which have opposing effects on dopaminergic transmission at a synaptic level, should also have somewhat different effects on striatal connectivity at the systems level of neuroimaging: sulpiride consistently increased striatal connectivity compared with placebo whereas methylphenidate less consistently and saliently tended to have the opposite effect. This observation, together with the relative lack of effect on striatal connectivity of non-dopaminergic drugs, suggests that the effects of sulpiride are indeed mediated by dopamine receptors and are not persuasively attributable to binding at other receptors or non-specific effects such as sedation.

It remains an intriguing question to consider how the effects of sulpiride on fMRI data could be related to the effects of dopaminergic drugs on electrophysiological recordings from rats, monkeys and patients with Parkinson’s disease. One simple notion is that enhanced connectivity of caudate following sulpiride may be a signature of the same dopaminergic effect as is indicated by increased low frequency coherence within and between CST circuits in parkinsonian animals and patients. However, there are clearly many points of difference between our experiment and those already published in the electrophysiological literature in terms of the anatomical regions studied, the sample characteristics, the dopaminergic manipulation and the modality of neurophysiological measurement. A more assertive statement about correspondence between drug effects on connectivity/coherence measured electrophysiologically and with fMRI will probably need to await future multimodal studies of monkey models or post-surgical patients with Parkinson’s disease.

In some electrophysiological studies, dopaminergic drugs modulated long-memory, low frequency or multisecond periodicities in spontaneous oscillations of basal ganglia neurons (Ruskin *et al.*, 1999; Walters *et al.*, 2000). There is preliminary evidence that human fMRI time series recorded ‘at rest’ can likewise demonstrate long-memory autocorrelations or 1/f noise (Zarahn *et al.*, 1997; Fadili and Bullmore, 2002) and that spatially distributed brain regions may be functionally connected to constitute so-called ‘resting state networks’

(RSNs) which demonstrate correlated low frequency fluctuations (Lowe *et al.*, 2000). Despite the different time scales of fMRI and electrophysiological measurements, one might argue that long memory structure is typically fractal or statistically self-similar and it is, therefore, unsurprising that it should be consistently observable over a range of time scales (Linkenkaer-Hansen *et al.*, 2001; Goldberger *et al.*, 2002). In any case, it would also be interesting in future to test the hypotheses that dopaminergic drug treatments may modulate not only connectivity between components of an activated CST system, as we have shown here, but may also affect the spectral properties of long memory fMRI noise and/or the strength of correlation between components of resting state networks.

Some methodological issues deserve comment. Several pharmacological MRI studies have described regionally segregated effects of drug challenge on brain function in young adults (Sell *et al.*, 1997; Gollub *et al.*, 1998; Honey *et al.*, 1999; Kimberg *et al.*, 2001). In this context, the present study has two main claims to innovation. First, we have chosen to measure drug effects on brain function in an unusually elderly sample. We were motivated to do so by a strategic interest in using pharmacological MRI to study age-related changes in brain function related to concomitant changes in neurotransmitter systems already well-described in animal models (Arnsten *et al.*, 1995). It has been shown in monkeys that pharmacological MRI can be used to map age-related changes in drug effects on brain function (Zhang *et al.*, 2001). As a first step in establishing the feasibility of this approach in humans, we wanted simply to demonstrate that it was possible to measure drug effects on neurocognitive function in healthy elderly participants. These results set the stage for future studies directly comparing drug effects on human neurocognitive function at different ages (as well as providing a basis for case-control studies of pharmacological effects on integrated brain function in elderly patient groups). However, until the results of such studies are known, it would be premature to assert that the pattern of drug effects we have reported here will be representative of all ages. It is more likely that drug effects are conditional on baseline activity and structural integrity of relevant transmitter systems, which are expected to change with age.

We should also consider the fact that the observed dopaminergic effects on physiological connectivity were not associated with change in response accuracy or reaction time. As well as removing the ambiguity that would attend the interpretation of a neurophysiological change in the face of a behavioural impairment, i.e. is the fMRI change produced by the behavioural alteration rather than drug, this suggests that the imaging provides a more sensitive measure of the drug effects than do the overt behavioural measures. This finding that is perhaps unsurprising given the fact that error rates and reaction times can remain unaltered even though the cognitive processes that generate them may change profoundly.

A final methodological point relates to the interpretation of positive and negative path coefficients in terms of excitatory and inhibitory synaptic transmission, respectively (Nyberg *et al.*, 1996). If this general rule was correct, then connections in our model which are known to be directly or indirectly mediated by inhibitory GABAergic transmission, such as caudate–thalamic connections, should be consistently described at a systems level by negative path coefficients and vice versa for known excitatory, glutamatergic projections, e.g. from cortex to caudate. However, this was not the case; which probably implies caution in supposing that the sign of a path coefficient is a simple, reliable indicator of the excitatory or inhibitory mode of synaptic events mediating connections between ensembles of neurons.

In summary, we have used pharmacological fMRI and multivariate data analysis methods to model integrated function of a CST system in humans and to confirm our hypothetical prediction that dopaminergic drugs would specifically modulate striatal connectivity.

Acknowledgments

We wish to thank the volunteers who participated in this study for their co-operation and the staff of the MRI Unit, Maudsley Hospital, London UK, for technical assistance. This work was supported by the Wellcome Trust and by an experimental medicine research grant from GlaxoSmithKline plc to E.T.B. and others. G.D.H. was supported by a University of Cambridge Pinsent–Darwin Fellowship in Mental Pathology.

Abbreviations

BFI	Bollen's parsimonious fit index
CST	cortico-striato-thalamic
fMRI	functional MRI
GABA	γ-aminobutyric acid
RMSEA	root mean square error of approximation

References

Afifi, AK.; Bergman, RA. Functional neuroanatomy: text and atlas. McGraw-Hill; London: 1998.

Alexander GE, DeLong MR, Strick PL. Parallel organization of functionally segregated circuits linking basal ganglia and cortex. Annu Rev Neurosci. 1986; 9:357–381. [PubMed: 3085570]

Alexander GE, Crutcher MD, DeLong RM. Basal gangliathalamocortical circuits: parallel substrates for motor, oculomotor, "prefrontal" and "limbic" functions. Prog Brain Res. 1990; 85:119–46. [PubMed: 2094891]

Arnsten AF, Cai JX, Steere JC, Goldman-Rakic PS. Dopamine D2 receptor mechanisms contribute to age-related cognitive decline: the effects of quinpirole on memory and motor performance in monkeys. J Neurosci. 1995; 15:3429–39. [PubMed: 7751922]

Bergman H, Feingold A, Nini A, Raz A, Slovin H, Abeles M, et al. Physiological aspects of information processing in the basal ganglia of normal and parkinsonian primates. Trends Neurosci. 1998; 21:32–8. [PubMed: 9464684]

Bollen, KA. Structural equations model with latent variables. Wiley; New York: 1989.

Brammer MJ, Bullmore ET, Simmons A, Williams SC, Grasby PM, Howard RJ, et al. Generic brain activation mapping in functional magnetic resonance imaging: a nonparametric approach. Magn Reson Imaging. 1997; 15:763–70. [PubMed: 9309607]

Brown P, Oliviero A, Mazzone P, Insola A, Tonali P, Di Lazzaro V. Dopamine dependency of oscillations between subthalamic nucleus and pallidum in Parkinson's disease. J Neurosci. 2001; 21:1033–8. [PubMed: 11157088]

Büchel C, Coull JT, Friston KJ. The predictive value of changes in effective connectivity for human learning. Science. 1999; 283:1538–41. [PubMed: 10066177]

Büchel C, Friston KJ. Modulation of connectivity in visual pathways by attention: cortical interactions evaluated with structural equation modelling and fMRI. Cereb Cortex. 1997; 7:768–78. [PubMed: 9408041]

Büchel C, Friston K. Assessing interactions among neuronal systems using functional neuroimaging. Neural Netw. 2000; 13:871–82. [PubMed: 11156198]

Bullmore E, Brammer M, Williams SC, Rabe-Hesketh S, Janot N, David A, et al. Statistical methods of estimation and inference for functional MR image analysis. Magn Reson Med. 1996; 35:261–77. [PubMed: 8622592]

Bullmore ET, Brammer MJ, Rabe-Hesketh S, Curtis VA, Morris RG, Williams SC, et al. Methods for diagnosis and treatment of stimulus-correlated motion in generic brain activation studies using fMRI. Hum Brain Mapp. 1999a; 7:38–48. [PubMed: 9882089]

Bullmore ET, Suckling J, Overmeyer S, Rabe-Hesketh S, Taylor E, Brammer MJ. Global, voxel, and cluster tests, by theory and permutation, for a difference between two groups of structural MR images of the brain. IEEE Trans Med Imaging. 1999b; 18:32–42. [PubMed: 10193695]

Bullmore E, Horwitz B, Honey G, Brammer M, Williams S, Sharma T. How good is good enough in path analysis of fMRI data? Neuroimage. 2000; 11:289–301. [PubMed: 10725185]

Bullmore E, Long C, Suckling J, Fadili J, Calvert G, Zelaya F, et al. Coloured noise and computational inference in neurophysiological (fMRI) time series analysis: resampling methods in time and wavelet domains. Hum Brain Mapp. 2001; 12:61–78. [PubMed: 11169871]

Bullmore E, Suckling J, Zelaya F, Long C, Honey G, Reed L, et al. Practice and difficulty evoke anatomically and pharmacologically dissociable brain activation dynamics. Cereb Cortex. 2003; 13:144–54. [PubMed: 12507945]

Chapman MA, See RE. Differential effects of unique profile antipsychotic drugs on extracellular amino acids in the ventral pallidum and globus pallidus of rats. J Pharmacol Exp Ther. 1996; 277:1586–94. [PubMed: 8667227]

Dermon CR, Barbas H. Contralateral thalamic projections predominantly reach transitional cortices in the rhesus monkey. J Comp Neurol. 1994; 344:508–31. [PubMed: 7523458]

Fadili MJ, Bullmore ET. Wavelet-generalized least squares: a new BLU estimator of linear regression models with 1/f errors. Neuroimage. 2002; 15:217–32. [PubMed: 11771991]

Friston KJ, Frith CD, Liddle PF, Frackowiak RS. Functional connectivity: the principal-component analysis of large (PET) data sets. J Cereb Blood Flow Metab. 1993; 13:5–14. [PubMed: 8417010]

Friston KJ, Buechel C, Fink GR, Morris J, Rolls E, Dolan RJ. Psychophysiological and modulatory interactions in neuroimaging. Neuroimage. 1997; 6:218–29. [PubMed: 9344826]

Friston K, Phillips J, Chawla D, Buchel C. Revealing interactions among brain systems with nonlinear PCA. Hum Brain Mapp. 1999; 8:92–7. [PubMed: 10524598]

Gerstein GL, Perkel DH. Simultaneously recorded trains of action potentials: analysis and functional interpretation. Science. 1969; 164:828–30. [PubMed: 5767782]

Gerstein GL, Bedenbaugh P, Aertsen AMHJ. Neuronal assemblies. IEEE Trans Biomed Eng. 1989; 36:4–14. [PubMed: 2646211]

Giguere M, Goldman-Rakic PS. Mediodorsal nucleus: areal, laminar, and tangential distribution of afferents and efferents in the frontal lobe of rhesus monkeys. J Comp Neurol. 1988; 277:195–213. [PubMed: 2466057]

Gitelman DR, Parrish TB, Friston KJ, Mesulam MM. Functional anatomy of visual search: regional segregations within the frontal eye fields and effective connectivity of the superior colliculus. Neuroimage. 2002; 15:970–82. [PubMed: 11906237]

Glymour, C.; Scheines, R.; Spirtes, P.; Kelly, K. Discovering causal structure: artificial intelligence, philosophy of science, and statistical modeling. Academic Press; New York: 1987.

Goldberger AL, Amaral LA, Hausdorff JM, Ivanov P, Peng CK, Stanley HE. Fractal dynamics in physiology: alterations with disease and aging. Proc Natl Acad Sci USA. 2002; 99(Suppl 1):2466–72. [PubMed: 11875196]

Gollub RL, Breiter HC, Kantor H, Kennedy D, Gastfriend D, Mathew RT, et al. Cocaine decreases cortical cerebral blood flow but does not obscure regional activation in functional magnetic resonance imaging in human subjects. J Cereb Blood Flow Metab. 1998; 18:724–34. [PubMed: 9663502]

Graybiel AM, Rauch SL. Toward a neurobiology of obsessive-compulsive disorder. Neuron. 2000; 28:343–7. [PubMed: 11144344]

Grimm JW, See RE. Unique activation of extracellular striatopallidal neurotransmitters in rats following acute risperidone. Brain Res. 1998; 801:182–9. [PubMed: 9729373]

Honey GD, Bullmore ET, Soni W, Varatheesan M, Williams SC, Sharma T. Differences in frontal cortical activation by a working memory task after substitution of risperidone for typical antipsychotic drugs in patients with schizophrenia. Proc Natl Acad Sci USA. 1999; 96:13432–7. [PubMed: 10557338]

Honey GD, Fu CHY, Kim J, Brammer MJ, Croudace TJ, Suckling J, et al. Effects of verbal working memory load on cortico-cortical connectivity modelled by path analysis of functional magnetic resonance imaging data. Neuroimage. 2002; 17:573–82. [PubMed: 12377135]

Horwitz B, Friston KJ, Taylor JG. Neural modeling and functional brain imaging: an overview. Neural Netw. 2000; 13:829–46. [PubMed: 11156195]

Ilinsky IA, Jouandet ML, Goldman-Rakic PS. Organization of the nigrothalamocortical system in the rhesus monkey. J Comp Neurol. 1985; 236:315–30. [PubMed: 4056098]

Jöreskog, KG.; Sörbom, D. LISREL 8 user's reference guide. Scientific Software International; Chicago: 1996.

Kievit J, Kuypers HGJM. Organization of the thalamo-cortical connections to the frontal lobe in the rhesus monkey. Exp Brain Res. 1977; 29:299–322. [PubMed: 410652]

Kim R, Nakano K, Jayaraman A, Carpenter MB. Projections of the globus pallidus and adjacent structures: an autoradiographic study in the monkey. J Comp Neurol. 1976; 169:263–90. [PubMed: 823180]

Kimberg DY, Aguirre GK, Lease J, D'Esposito M. Cortical effects of bromocriptine, a D-2 dopamine receptor agonist, in human subjects, revealed by fMRI. Hum Brain Mapp. 2001; 12:246–57. [PubMed: 11241875]

Lawrence AD, Sahakian BJ, Robbins TW. Cognitive functions and corticostriatal circuits: insights from Huntington's disease. Trends Cogn Sci. 1998; 2:379–88. [PubMed: 21227253]

Lawrie SM, Büchel C, Whalley HC, Frith CD, Friston KJ, Johnstone EC. Reduced frontotemporal functional connectivity in schizophrenia associated with auditory hallucinations. Biol Psychiatry. 2002; 51:1008–11. [PubMed: 12062886]

Linkenkaer-Hansen K, Nikouline VV, Palva JM, Ilmoniemi RJ. Long-range temporal correlations and scaling behavior in human brain oscillations. J Neurosci. 2001; 21:1370–7. [PubMed: 11160408]

Loehlin, JC. Latent variable models: an introduction to factor, path and structural analysis. Lawrence Erlbaum; Hillsdale (NJ): 1987.

Lowe MJ, Dzemidzic M, Lurito JT, Mathews VP, Phillips MD. Correlations in low-frequency BOLD fluctuations reflect corticocortical connections. Neuroimage. 2000; 12:582–7. [PubMed: 11034865]

Masterman DL, Cummings JL. Frontal-subcortical circuits: the anatomic basis of executive, social and motivated behaviors. J Psychopharmacol. 1997; 11:107–14. [PubMed: 9208374]

McGuire PK, Bates JF, Goldman-Rakic PS. Interhemispheric integration: I. Symmetry and convergence of the corticocortical connections of the left and the right principal sulcus (PS) and the left and the right supplementary motor area (SMA) in the rhesus monkey. Cereb Cortex. 1991; 1:390–407. [PubMed: 1726605]

McIntosh AR, Grady CL, Ungerleider LG, Haxby JV, Rapoport SI, Horwitz B. Network analysis of cortical visual pathways mapped with PET. J Neurosci. 1994; 14:655–66. [PubMed: 8301356]

McIntosh AR, Grady CL, Haxby JV, Ungerleider LG, Horwitz B. Changes in limbic and prefrontal functional interactions in a working memory task for faces. Cereb Cortex. 1996; 6:571–84. [PubMed: 8670683]

Mechelli A, Penny WD, Price CJ, Gitelman DR, Friston KJ. Effective connectivity and intersubject variability: using a multisubject network to test differences and commonalities. Neuroimage. 2002; 17:1459–69. [PubMed: 12414285]

Mega, MS.; Cummings, JL. Frontal subcortical circuits: anatomy and function. In: Salloway, SP.; Malloy, PF.; Duffy, JD., editors. The frontal lobes and neuropsychiatric illness. American Psychiatric Publishing; London: 2001. p. 15-33.

Nyberg L, McIntosh AR, Cabeza R, Nilsson LG, Houle S, Habib R, et al. Network analysis of positron emission tomography regional cerebral blood flow data: ensemble inhibition during episodic memory retrieval. J Neurosci. 1996; 16:3753–9. [PubMed: 8642418]

Opacka-Juffry J, Ashworth S, Ahier RG, Hume SP. Modulatory effects of L-DOPA on D2 dopamine receptors in rat striatum, measured using in vivo microdialysis and PET. J Neural Transm. 1998; 105:349–64. [PubMed: 9720967]

Overmeyer S, Bullmore ET, Suckling J, Simmons A, Williams SC, Santosh PJ, et al. Distributed grey and white matter deficits in hyperkinetic disorder: MRI evidence for anatomical abnormality in an attentional network. Psychol Med. 2001; 31:1425–35. [PubMed: 11722157]

Owen AM, James M, Leigh PN, Summers BA, Marsden CD, Quinn NP, et al. Fronto-striatal cognitive deficits at different stages of Parkinson's disease. Brain. 1992; 115:1727–51. [PubMed: 1486458]

Pandya DN, Yeterian EH. Prefrontal cortex in relation to other cortical areas in rhesus monkey: architecture and connections. Prog Brain Res. 1990; 85:63–94. [PubMed: 2094916]

Pantelis C, Barnes TR, Nelson HE, Tanner S, Weatherley L, Owen AM, et al. Frontal-striatal cognitive deficits in patients with chronic schizophrenia. Brain. 1997; 120:1823–43. [PubMed: 9365373]

Parent A, Bouchard C, Smith Y. The striatopallidal and striatonigral projections: two distinct fiber systems in primate. Brain Res. 1984; 303:385–90. [PubMed: 6744030]

Raz A, Vaadia E, Bergman H. Firing patterns and correlations of spontaneous discharge of pallidal neurons in the normal and the tremulous 1-methyl-4-phenyl-1,2,3,6-tetrahydropyridine vervet model of parkinsonism. J Neurosci. 2000; 20:8559–71. [PubMed: 11069964]

Raz A, Frechter-Mazar V, Feingold A, Abeles M, Vaadia E, Bergman H. Activity of pallidal and striatal tonically active neurons is correlated in MPTP-treated monkeys but not in normal monkeys. J Neurosci. 2001; 21:RC128. [PubMed: 11157099]

Robbins TW. The case of frontostriatal dysfunction in schizophrenia. Schizophr Bull. 1990; 16:391–402. [PubMed: 2287930]

Rowe J, Stephan KE, Friston K, Frackowiak R, Lees A, Passingham R. Attention to action in Parkinson's disease: impaired effective connectivity among frontal cortical regions. Brain. 2002; 125:276–89. [PubMed: 11844728]

Ruskin DN, Bergstrom DA, Walter JR. Multisecond oscillations in firing rate in globus pallidus: synergistic modulation by D1 and D2 dopamine receptors. J Pharmacol Exp Ther. 1999; 290:1493–501. [PubMed: 10454529]

Selemon LD, Goldman-Rakic PS. Longitudinal topography and interdigitation of corticostriatal projections in the rhesus monkey. J Neurosci. 1985; 5:776–94. [PubMed: 2983048]

Sell LA, Simmons A, Lemmens GM, Williams SC, Brammer M, Strang J. Functional magnetic resonance imaging of the acute effect of intravenous heroin administration on visual activation in long-term heroin addicts: results from a feasibility study. Drug Alcohol Depend. 1997; 49:55–60. [PubMed: 9476700]

Talairach, J.; Tournoux, P. Co-planar stereotaxic atlas of a human brain. Thieme Verlag; Stuttgart: 1988.

Toni I, Rowe J, Stephan KE, Passingham RE. Changes of corticostriatal effective connectivity during visuomotor learning. Cereb Cortex. 2002; 12:1040–7. [PubMed: 12217967]

Venables, WN.; Ripley, BD. Modern applied statistics with S-PLUS. 4th ed. Springer Verlag; New York: 2002.

Walters JR, Ruskin DN, Allers KA, Bergstrom DA. Pre- and postsynaptic aspects of dopamine-mediated transmission. Trends Neurosci. 2000; 23(10 Suppl):S41–7. [PubMed: 11052219]

Welchew DE, Honey GD, Sharma T, Robbins TW, Bullmore ET. Mulitidimensional scaling of integrated neurocognitive function and schizophrenia as a disconnexion disorder. Neuroimage. 2002; 17:1227–39. [PubMed: 12414263]

Wichmann T, DeLong MR. Functional and pathophysiological models of the basal ganglia. Curr Opin Neurobiol. 1996; 6:751–8. [PubMed: 9000030]

Williams D, Tijssen M, Van Bruggen G, Bosch A, Insola A, Di Lazzaro V, et al. Dopamine-dependent changes in the functional connectivity between basal ganglia and cerebral cortex in humans. Brain. 2002; 125:1558–69. [PubMed: 12077005]

Worsley KJ, Cao J, Paus T, Petrides M, Evans AC. Applications of random field theory to functional connectivity. Hum Brain Mapp. 1998; 6:364–7. [PubMed: 9788073]

Wright IC, Sham P, Murray RM, Weinberger DR, Bullmore ET. Genetic contributions to regional variability in human brain structure: methods and preliminary results. Neuroimage. 2002; 17:256–71. [PubMed: 12482082]

Zarahn E, Aguirre GK, D'Esposito M. Empirical analyses of BOLD fMRI statistics. I. Spatially unsmoothed data collected under null-hypothesis conditions. Neuroimage. 1997; 5:179–97. [PubMed: 9345548]

Zhang Z, Anderson A, Grondin R, Bauber T, Avison R, Gerhardt G, et al. Pharmacological MRI mapping of age-associated changes in basal ganglia circuitry of awake rhesus monkeys. Neuroimage. 2001; 14:1159–67. [PubMed: 11697947]

Europe PMC Funders Author Manuscripts

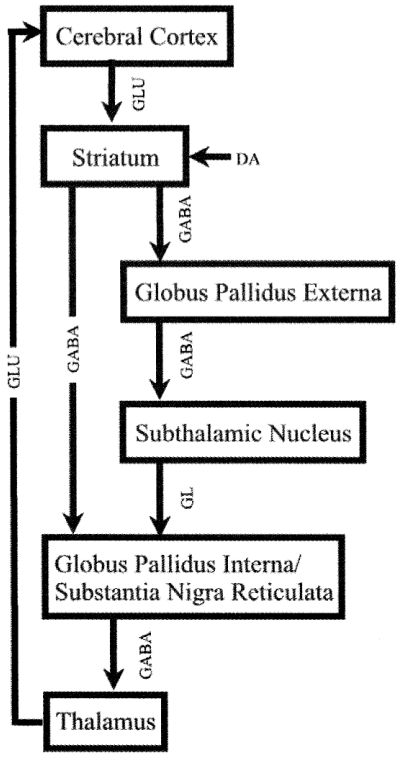

Fig. 1.

Schematic illustration of CST circuitry (Alexander *et al.*, 1986). Each of five circuits originates with an efferent excitatory (glutamatergic) projection from one of several frontal cortical areas to caudate nucleus, putamen or ventral striatum. Direct or indirect routes connect these input nuclei of the basal ganglia to globus pallidus. From globus pallidus, there is an inhibitory (GABAergic) connection to thalamus; from thalamus, a glutamatergic projection returns to the cortical area that issued the original efferent projection to basal ganglia. DA = dopamine; GLU = glutamate; GL = glutamine; GABA = γ-aminobutyric acid; DLPFC = dorsolateral prefrontal cortex.

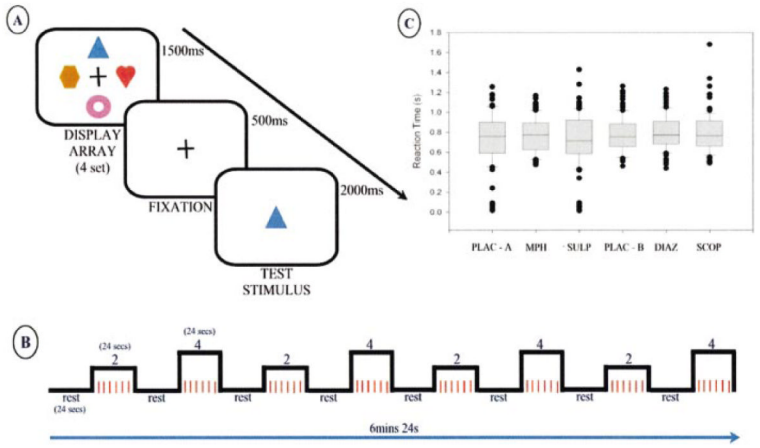

Fig. 2.

Object location learning trials. (**A**) Stimuli and target presentation. (**B**) Blocked trials of alternating periods of fixation (rest) and object location learning (six trials per block) at two different levels of difficulty (two or four stimuli presented). (**C**) Box plot of response latencies across treatment conditions. PLAC-A = placebo (group A); MPH = methylphenidate; SULP = sulpiride; PLAC-B = placebo (group B); DIAZ = diazepam; SCOP = scopolamine.

Europe PMC Funders Author Manuscripts

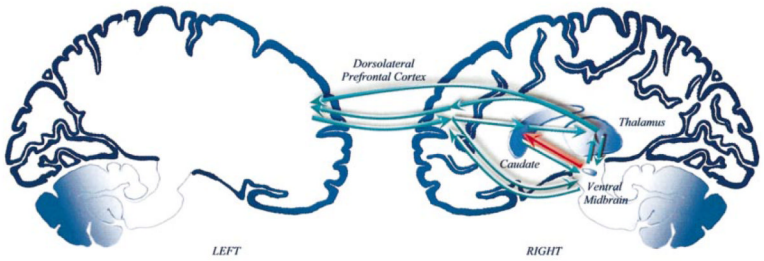

Fig. 3.

Path model specification. Arrows indicate modelled directional inter-regional effective connections within the prefronto-striatonigro-thalamic circuit. The most salient effect of drug treatment, highlighted by the red arrow, was dopaminergic modulation of the effective connection from ventral midbrain to caudate nucleus.

Europe PMC Funders Author Manuscripts

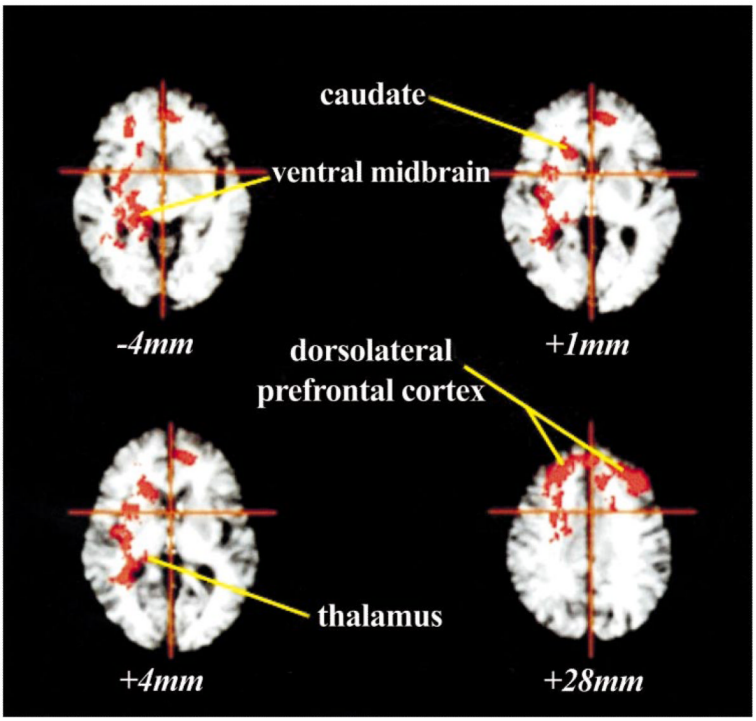

Fig. 4.

Generic brain activation maps Highlighted voxels indicate areas of significant response to the load manipulation in the object–location learning task over all subjects following placebo treatment ($n = 23$). Activated regions involve the CST system. The distance of each map above the intercommissural line in the standard space of Talairach and Tournoux (1988) is given in millimeters; the red crosshair locates the origin of the x and y coordinates in each slice. In accordance with radiological convention, the right side of the brain is shown on the left side of each map.

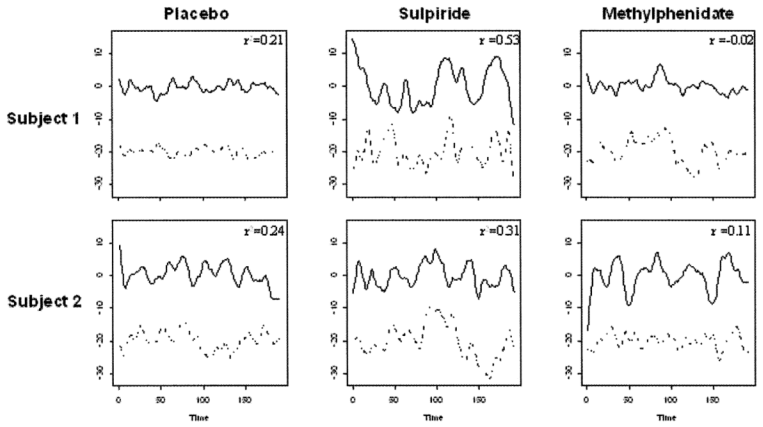

Fig. 5.

fMRI time series from the caudate nucleus (solid line) and the ventral midbrain (dotted line) in two individual subjects scanned following placebo and dopaminergic (sulpiride and methylphenidate) drug treatments. r^2 values indicating the percentage of variance in each time series accounted for by their correlation are inset for each panel.

Europe PMC Funders Author Manuscripts

Europe PMC Funders Author Manuscripts

Table 1

Functional connectivity between brain regions in fMRI data acquired following placebo treatment (n = 23)

	Caudate	Thalamus	Ventral midbrain	Left dorsolateral prefrontal cortex	Right dorsolateral prefrontal cortex
Caudate	3.16	0.561	0.641	0.658	1.395
Thalamus	0.195	2.607	1.348	−0.227	1.103
Ventral midbrain	0.216	0.5	2.787	0.134	0.822
Left dorsolateral prefrontal cortex	0.221	−0.084	0.048	2.809	1.165
Right dorsolateral prefrontal cortex	0.426	0.371	0.267	0.377	3.395
Residual variances	2.726	2.312	2.45	2.466	2.894

Sample correlations are shown below the diagonal; sample variances and covariances are shown on and above the diagonal. Residual variances are estimated by principal component analysis (Honey *et al.*, 2002) and indicate the variance in each region that is not accounted for by connectivity with other regions.

Brain. Author manuscript; available in PMC 2013 November 25.

Europe PMC Funders Author Manuscripts

Table 2

Linear mixed effects modelling of inter-regional correlation coefficients

	Group A					Group B				
	Intercept		Drug effects			Intercept		Drug effects		
Regional correlation	μ (SE)	*P* value (corrected)	Methylphenidate β (SE)	Sulpiride β (SE)	*P* value (corrected)	μ (SE)	*P* value (corrected)	Diazepam β (SE)	Scopolamine β (SE)	*P* value (corrected)
CD/VPT	0.28 (0.07)	0.0001 (0.015)	0.01 (0.07)	0.22 (0.07)	0.0017 (0.025)	0.28 (0.07)	0.0001 (0.015)	0.03 (0.06)	0.13 (0.07)	0.1015
CD/VMB	0.3 (0.06)	0.0001 (0.015)	−0.08 (0.06)	0.12 (0.06)	0.0038 (0.057)	0.3 (0.07)	0.0001 (0.015)	−0.02 (0.06)	0.04 (0.06)	0.6532
CD/LPFC	0.14 (0.07)	0.0001 (0.015)	−0.02 (0.07)	0.09 (0.08)	0.3253	0.24 (0.08)	0.0001 (0.015)	0.06 (0.09)	0.03 (0.09)	0.7825
CD/RPFC	0.38 (0.08)	0.0001 (0.015)	0.06 (0.1)	0.05 (0.1)	0.7702	0.43 (0.09)	0.0001 (0.015)	−0.14 (0.09)	0.08 (0.09)	0.0298 (0.447)
VPT/VMB	0.78 (0.08)	0.0001 (0.015)	0.06 (0.09)	0.13 (0.09)	0.3207	0.93 (0.12)	0.0001 (0.015)	0.03 (0.08)	0.21 (0.08)	0.0189 (0.283)
VPT/LPFC	0.25 (0.06)	0.0001 (0.015)	0.04 (0.08)	0.02 (0.08)	0.8471	0.35 (0.07)	0.0001 (0.015)	−0.02 (0.07)	−0.05 (0.07)	0.7713
VPT/RPFC	0.27 (0.07)	0.0001 (0.015)	0.09 (0.08)	0.07 (0.08)	0.5117	0.35 (0.06)	0.0001 (0.015)	0.01 (0.06)	0.11 (0.6)	0.1037
VMB/LPFC	0.21 (0.06)	0.0001 (0.015)	−0.001 (0.06)	−0.01 (0.06)	0.9686	0.32 (0.07)	0.0001 (0.015)	0.03 (0.07)	−0.05 (0.07)	0.5053
VMB/RPFC	0.23 (0.06)	0.0001 (0.015)	0.04 (0.08)	0.03 (0.08)	0.8337	0.28 (0.06)	0.0001 (0.015)	0.09 (0.05)	0.13 (0.05)	0.0601
LPFC/RPFC	0.36 (0.06)	0.0001 (0.015)	0.11 (0.06)	0.08 (0.07)	0.1733	0.49 (0.09)	0.0001 (0.015)	0.17 (0.1)	0.07 (0.1)	0.2015

A model treating drug and load as fixed effects and subject as a random effect (Eqn 2) was fitted to the individually estimated inter-regional correlation coefficients in each treatment group. The intercept (μ) indicates the mean value of the correlation coefficient under all drug (and load) conditions; the main effect of drug indicates the probability of the observed between drug difference for each correlation in each group; the coefficients (β) for each drug indicate their effect on each correlation compared to placebo. *P* values <0.05 are also reported (in parentheses after correction for multiple comparisons by a Bonferroni procedure). CD = caudate; LPFC = left dorsolateral prefrontal cortex; RPFC = right dorsolateral prefrontal cortex; VMB = ventral midbrain; VPT = ventro-posterior thalamus; SE = standard error.

Europe PMC Funders Author Manuscripts

Brain. Author manuscript; available in PMC 2013 November 25.

Table 3

Linear mixed effects modelling of inter-regional path coefficients

	Group A					Group B				
	Intercept		Drug effects			Intercept		Drug effects		
Path coefficients	μ (SE)	*P* value (corrected)	Methylphenidate β (SE)	Sulpiride β (SE)	*P* value (corrected)	μ (SE)	*P* value (corrected)	Diazepam β (SE)	Scopolamine β (SE)	*P* value (corrected)
VMB → CD	0.16 (0.06)	0.0001 (0.015)	−0.05 (0.06)	0.15 (0.06)	0.0021 (0.031)	0.21 (0.06)	0.0001 (0.015)	−0.002 (0.06)	−0.07 (0.06)	0.4698
RPFC → CD	0.31 (0.07)	0.0001 (0.015)	0.03 (0.08)	−0.02 (0.08)	0.81	0.32 (0.08)	0.0001 (0.015)	−0.15 (0.08)	0.05 (0.08)	0.0364 (0.54)
CD → VPT	0.09 (0.05)	0.0005 (0.075)	0.02 (0.05)	0.05 (0.05)	0.67	0.04 (0.04)	0.0022 (0.033)	0.07 (0.04)	0.07 (0.04)	0.2213
VMB → VPT	0.34 (0.03)	0.0001 (0.015)	0.009 (0.04)	0.003 (0.04)	0.97	0.35 (0.04)	0.0001 (0.015)	−0.03 (0.04)	0.05 (0.04)	0.1236
CD → VMB	0.04 (0.05)	0.9407	−0.054 (0.06)	−0.16 (0.06)	0.0234 (0.351)	−0.02 (0.05)	0.024 (0.36)	−0.01 (0.05)	−0.02 (0.05)	0.9225
VPT → VMB	0.38 (0.05)	0.0001 (0.015)	0.04 (0.06)	0.15 (0.06)	0.0383 (0.574)	0.45 (0.07)	0.0001 (0.015)	0.04 (0.05)	0.18 (0.05)	0.0046 (0.07)
RPFC → VMB	0.07 (0.04)	0.0301	−0.04 (0.05)	−0.02 (0.04)	0.6759	0.09 (0.05)	0.1204	0.04 (0.08)	−0.12 (0.08)	0.1016
VPT → LPFC	0.17 (0.05)	0.0001 (0.015)	−0.009 (0.06)	−0.005 (0.06)	0.9892	0.25 (0.05)	0.0001 (0.015)	−0.06 (0.05)	−0.09 (0.05)	0.1954
RPFC → LPFC	0.16 (0.03)	0.0001 (0.015)	0.07 (0.03)	0.05 (0.03)	0.0668	0.22 (0.04)	0.0001 (0.015)	0.09 (0.05)	0.02 (0.05)	0.1605
VPT → RPFC	0.18 (0.07)	0.0001 (0.015)	0.03 (0.08)	0.09 (0.08)	0.5444	0.28 (0.11)	0.0034 (0.051)	0.03 (0.14)	−0.13 (0.14)	0.4557
VMB → RPFC	−0.01 (0.09)	0.7102	0.03 (0.11)	−0.005 (0.11)	0.9294	−0.05 (0.013)	0.2795	−0.07 (0.16)	0.23 (0.16)	0.1629
LPFC → RPFC	0.20 (0.04)	0.0001 (0.015)	0.04 (0.04)	0.03 (0.04)	0.6433	0.23 (0.05)	0.0001 (0.015)	0.08 (0.05)	0.03 (0.05)	0.2668

A model treating drug and load as fixed effects and subject as a random effect (Eqn 2) was fitted to the individually estimated inter-regional correlation coefficients in each treatment group. The intercept (μ) indicates the mean value of the correlation coefficient under all drug (and load) conditions; the main effect of drug indicates the probability of the observed between drug difference for each correlation in each group; the coefficients (β) for each drug indicate their effect on each correlation compared to placebo. *P* values <0.05 are also reported (in parentheses after correction for multiple comparisons by a Bonferroni procedure). CD = caudate; LPFC = left dorsolateral prefrontal cortex; RPFC = right dorsolateral prefrontal cortex; VMB = ventral midbrain; VPT = ventro-posterior thalamus; SE = standard error.